OXFORD

Systems Biology

Biphasic regulation of transcriptional surge generated by the gene feedback loop in a two-component system

Wen Liu[1], Xiang Li[1,2], Hong Qi[3], Yuning Wu[1], Jing Qu[1], Zhiyong Yin[1], Xuejuan Gao[1], Aidong Han[2,4],* and Jianwei Shuai ⓘ [1,2,5],*

[1]Research Institute for Biomimetics and Soft Matter, Fujian Provincial Key Lab for Soft Functional Materials Research, Department of Physics, Xiamen University, Xiamen 361005, China, [2]State Key Laboratory of Cellular Stress Biology, Innovation Center for Cell Signaling Network, Xiamen University, Xiamen 361102, China, [3]Complex Systems Research Center, Shanxi University, Taiyuan 030006, China, [4]School of Life Sciences, Xiamen University, Xiamen 361102, China and [5]National Institute for Data Science in Health and Medicine, Xiamen University, Xiamen 361102, China

*To whom correspondence should be addressed.
Associate Editor: Jinbo Xu

Abstract

Motivation: Transcriptional surges generated by two-component systems (TCSs) have been observed experimentally in various bacteria. Suppression of the transcriptional surge may reduce the activity, virulence and drug resistance of bacteria. In order to investigate the general mechanisms, we use a PhoP/PhoQ TCS as a model system to derive a comprehensive mathematical modeling that governs the surge. PhoP is a response regulator, which serves as a transcription factor under a phosphorylation-dependent modulation by PhoQ, a histidine kinase.

Results: Our model reveals two major signaling pathways to modulate the phosphorylated PhoP (P-PhoP) level, one of which promotes the generation of P-PhoP, while the other depresses the level of P-PhoP. The competition between the P-PhoP-promoting and the P-PhoP-depressing pathways determines the generation of the P-PhoP surge. Furthermore, besides PhoQ, PhoP is also a bifunctional modulator that contributes to the dynamic control of P-PhoP state, leading to a biphasic regulation of the surge by the gene feedback loop. In summary, the mechanisms derived from the PhoP/PhoQ system for the transcriptional surges provide a better understanding on such a sophisticated signal transduction system and aid to develop new antimicrobial strategies targeting TCSs.

Availability and implementation: https://github.com/jianweishuai/TCS.

Contact: jianweishuai@xmu.edu.cn or ahan@xmu.edu.cn

Supplementary information: Supplementary data are available at *Bioinformatics* online.

1 Introduction

Two-component systems (TCSs), sophisticated signal transduction pathways in bacteria (Hess *et al.*, 1988; Ninfa and Magasanik, 1986), eubacteria, archaea and plants (Chang and Stewart, 1998; Perraud *et al.*, 1999), are responsible for over 90% signal transduction processes in response to extracellular stimuli, such as nutrient availability, osmolarity, redox state, temperature and toxic chemicals (Robinson et al., 2000; Stock *et al.*, 2000; Wuichet et al., 2010). TCSs are not found in mammalian cells, and thus considered as potential targets for new antimicrobial drugs (Wuichet *et al.*, 2010).

A prototypical TCS consists of two conserved protein components, a sensor histidine kinase (HK) and a cognate response regulator (RR). In general, HK is a transmembrane protein to sense extracellular signals (Krell *et al.*, 2010; Mascher *et al.*, 2006), including cell density (Pestova *et al.*, 1996), environmental

conditions, such as nitrate (Williams and Stewart, 1997), divalent cations including magnesium and calcium (Groisman, 2001), oxygen (Jason *et al.*, 2007), and so on. Upon stimuli, HK becomes autophosphorylated at a conserved histidine residue in the presence of adenosine triphosphate (ATP) to form the phosphorylated HK (P-HK) that then transfers the phosphoryl group to an aspartate residue in the receiver domain of its cognate RR, generating a phosphorylated RR (P-RR). About two-third RRs preferably bind to a specific set of promoter DNA to regulate the expression of target genes (Gao *et al.*, 2007). Furthermore, the bifunctional HK exhibits intrinsic phosphatase activity to dephosphorylate its cognate P-RR(Igo *et al.*, 1989; Stock *et al.*, 2000; Straube, 2014), which is largely enhanced with the presence of adenosine diphosphate (ADP) and stimulation (Castelli *et al.*, 2000; Igo *et al.*, 1989).

The transcriptional surge is an important character of TCS families for various physiological functions (Alloing *et al.*, 1998; Guckes

et al., 2017; Hutchings *et al.*, 2006; Shin et al., 2006; Yamamoto and Ishihama, 2005). Upon stimulations, the levels of P-RR and transcription of the relevant genes rapidly increase to a peak, and then reduce to a steady-state that is approximately 20% to 50% of the maximum level, forming a surge (Shin *et al.*, 2006). Generally, adaptation is defined as a process where a system initially responds to the stimulus, and then returns to basal or near-basal level of activity in the cell signaling (Ferrell, 2016). Hence, the surge can be considered as an adaptable functionality in TCSs (Ray and Igoshin, 2010). When stimulated by a competence-stimulating peptide (CSP) in human pathogen *Streptococcus pneumonia*, the expression of comCDE mRNA exhibits a transient surge and plays a role in quorum sensing through a TCS ComD/ComE (Alloing *et al.*, 1998). The surge expression of copper-responsive genes of *Escherichia coli* is associated with the electron transport, reduction of nitrite and nitrous oxides, and electron carriers (Yamamoto and Ishihama, 2005). The surge can also regulate the vancomycin resistance by a TCS VanR/VanS in *Streptomyces coelicolor* (Hutchings *et al.*, 2006) and jump-start virulence circuit by a TCS PhoP/PhoQ in pathogenic *Salmonella enterica* (Shin *et al.*, 2006).

In 2006, Shin et al reported the activation surge in PhoP/PhoQ TCS with a positive feedback loop, which can regulate the pathogenicity in *Salmonella*. They studied two isogenic strains, i.e. the wild-type strain harboring the PhoP box that is responsible for transcriptional autoregulation and the mutant strain in which PhoP box was replaced by a consensus -35 sequence. When the wild-type strain was shifted from the medium containing 10mM Mg^{2+} to the inducing condition of $50\mu M$ Mg^{2+}, the level of PhoP continuously increased from a very low initial value, and the transcription of PhoP-activated genes showed an activation surge. While, the mutant strain produced the PhoP protein constitutively at levels that were similar to the steady-state level achieved by the wild-type strain after the induction of the PhoP/PhoQ system, and the transcription of PhoP-activated genes presented a monotonic increase and then asymptotically reached a steady-state level (Shin *et al.*, 2006).

Mathematical modeling is a powerful approach for dissecting the complexity, often providing new insights of the signaling pathways (Li *et al.*, 2020; 2021; Qi *et al.*, 2015, 2018). Several molecular mechanisms for the surge generation by TCSs were proposed with mathematical modeling (Mitrophanov *et al.*, 2010; Ray and Igoshin, 2010; Yeo *et al.*, 2012). Mitrophanov et al (Mitrophanov *et al.*, 2010) and Ray et al (Ray and Igoshin, 2010) discussed the surge phenomenon with TCS models considering the positive DNA feedback loop based on simple TCS system (Batchelor and Goulian, 2003). Yeo et al suggested that the surge modulated by ADP binding generates a negative feedback loop by upregulating the phosphatase activity of PhoQ (Yeo *et al.*, 2012).

Because none of the present models is able to systematically explain the experimental observations in the PhoP/PhoQ system (Batchelor and Goulian, 2003; Mitrophanov *et al.*, 2010; Ray and Igoshin, 2010; Shin *et al.*, 2006; Yeo *et al.*, 2012), we integrated the characteristics of the previous models (Batchelor and Goulian, 2003; Mitrophanov *et al.*, 2010; Ray and Igoshin, 2010; Yeo *et al.*, 2012), and constructed a complete TCS model to simulate the experiments (Shin *et al.*, 2006; Yeo *et al.*, 2012) and especially explained the mechanism that the wild-type strain produced a surge while the mutant strain did not. We further identified two major signaling pathways in the P-PhoP modulation, one of which promotes the generation of the P-PhoP, while the other decreases the level of P-PhoP. Therefore, the competition of these two pathways governs the P-PhoP level, resulting in the P-PhoP surge. Besides PhoQ, our model suggests that PhoP plays a bifunctional role in the P-PhoP generation, causing a biphasic regulation of the P-PhoP surge by the gene feedback loop.

2 Mathematical model

PhoP/PhoQ is used as a TCS model, because a positive feedback was observed when P-PhoP bound its promoter DNA to increase expression of PhoP and PhoQ in the wild-type strain, but not in a mutant strain (Shin *et al.*, 2006). This PhoP/PhoQ model is composed of four processes: the activation of PhoQ, the PhoP/PhoQ reactions, the PhoP binding to DNA and the gene transcription and translation.

The autokinase activity of PhoQ is repressed at greater than millimolar magnesium concentration ($\sim$10mM) and induced at low Mg^{2+} ($\sim$50μM) in *S. enterica* (Castelli *et al.*, 2000; Garcia Vescovi *et al.*, 1996). Because the observations of strains were shifted from media with 10mM to 50 μM Mg^{2+} concentrations in the experiments (Shin *et al.*, 2006), we assume that ATP or ADP could barely bind PhoQ in the presence of 10mM Mg^{2+}. When shifted to $50\mu M$ Mg^{2+}, PhoQ easily associates with ATP or ADP. And then PhoQ autophosphorylates to produce P-PhoQ and P-PhoQ-ADP in the induced condition, which further generates P-PhoP through their phosphotransferase activity (Dutta *et al.*, 1999) (Fig. 1A and B). Moreover, PhoQ and PhoQ-ADP possess a phosphatase activity that turns P-PhoP to PhoP through dephosphorylation (Castelli *et al.*, 2000; Yeo *et al.*, 2012).

There are two promoters to regulate the expression of PhoP and PhoQ, the regulated promoter and the constitutive promoter (Kato *et al.*, 1999; Lejona *et al.*, 2003; Yamamoto et al., 2002). The constitutive promoter is responsible for the production of basal levels of PhoP and PhoQ, which is necessary to detect and respond to environment signals (Shin and Groisman, 2005). And the major difference between the wild-type and mutant strains is the regulated promoter (Shin *et al.*, 2006). In the wild-type model, two RR-boxes 'X' and 'X#' can be bound with PhoP or P-PhoP. And only when bound by P-PhoP, the RR-boxes can promote the transcriptions of phoP/phoQ and pmrD genes, which are further translated into the relevant proteins (Fig. 1C and D). However, in the mutant model, the PhoP and PhoQ proteins can be produced constantly, because the RR-box is replaced by a consensus hexameric -35 sequence (Shin *et al.*, 2006) (Fig. 1D).

We determined the model parameters by fitting all the experimental data of P-PhoP level, the occupancy of pmrD promoter and mRNA expression of pmrD (Shin *et al.*, 2006). Both the wild-type and mutant models first show a steady state of inhibition (Fig. 1E–G). In the induced condition with $[Mg^{2+}] = 50\mu M$ at t = 0, the binding abilities of PhoQ to ATP and ADP increase significantly. PhoQ becomes autophosphorylated, leading to a P-PhoP surge in the wild-type strain (Fig. 1E, with the experimental data extracted from Fig. 2C of Shin *et al.*, 2006). The surge height H, the difference between the maximum and the final equilibrium concentrations of the P-PhoP level, is derived. The occupancy of the pmrD promoter (Fig. 1F, with the experimental data extracted from the lower panel of Fig. 3C in Shin *et al.*, 2006), the ratio of the probability of DNA bound by P-PhoP and PhoP to the probability of free DNA, i.e. $(p_1+p_2)/p_0$, shows a surge behavior along with the mRNA expression of pmrD ($mRNA_{(pmrD)}$) in wild-type model, rather than in mutant model (Fig. 1G, with experimental data extracted from the lower panel of Fig. 3D in Shin *et al.*, 2006). Both wild-type and mutant models can nicely recapitulate the experimental data with a small enough error.

All equations and parameter values are given in Supplementary Method S2 and Supplementary Table S1, respectively. The initial values (Supplementary Table S2) are assigned to the steady state of the model at 10mM Mg^{2+}. Furthermore, the initial concentrations of PhoP and PhoQ in the wild-type strain are approximately 2.7μM and 0.49μM, respectively, as measured by experiments (Yeo *et al.*, 2012). The initial value of PhoP in the mutant strain is similar to the steady state of the wild-type model at $50\mu M$ Mg^{2+} (Shin *et al.*, 2006).

3 Results

3.1 The dynamics of the three stages of the surge observed in wild-type strain

We focus on the surge of P-PhoP in the following discussions, because the changes in transcriptional level of PhoP-activated genes reflect the change of P-PhoP level (Shin *et al.*, 2006). As shown by solid lines in Figure 2A and B, the P-PhoP surge can be divided into
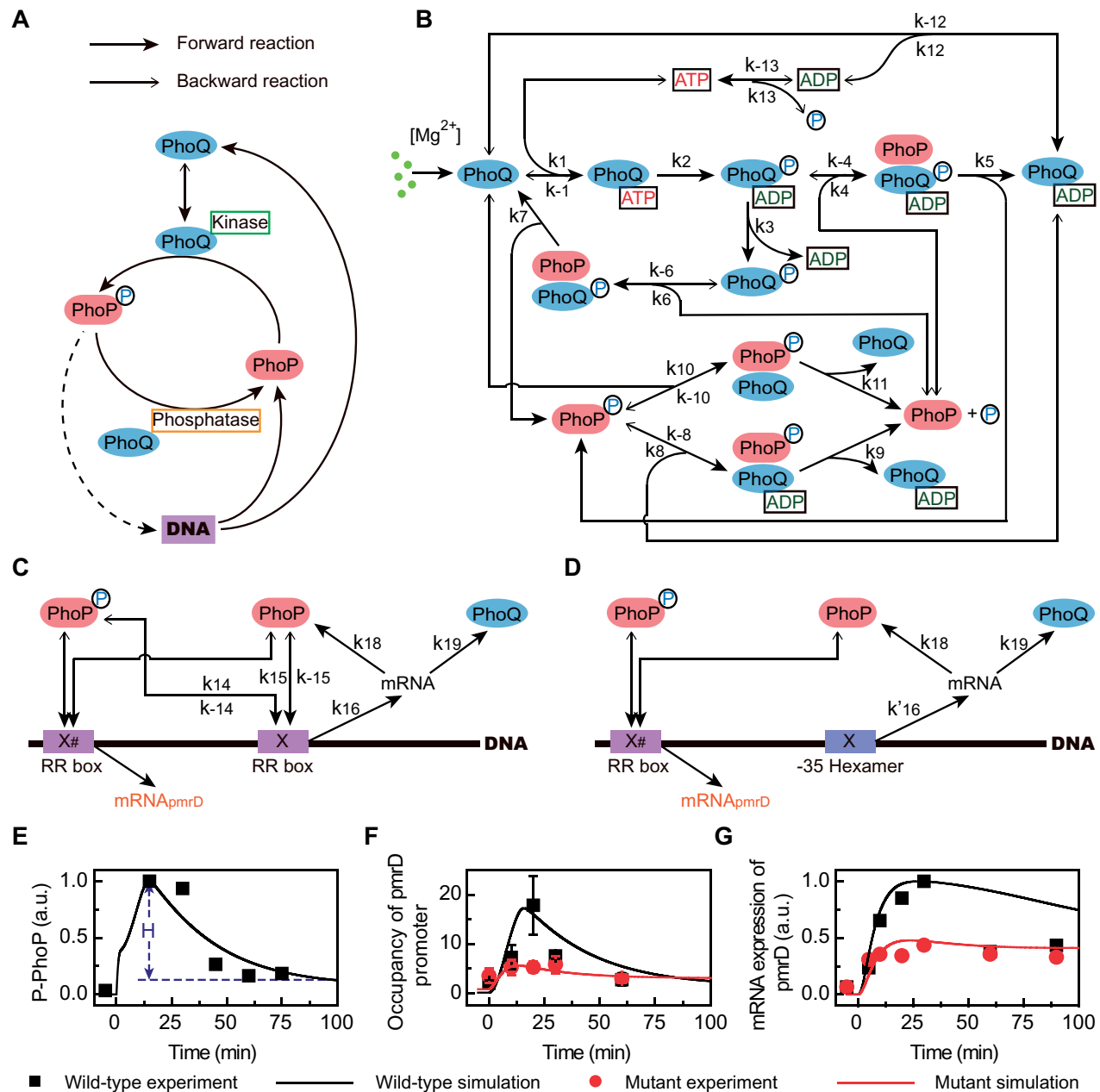
Fig. 1. Construction of the TCS PhoP/PhoQ model. (**A**) Simplified signal transduction of PhoP/PhoQ. The dashed line indicates the binding of P-PhoP with DNA in the wild-type but not in a mutant strain. (**B**) Detailed signal transduction of PhoP/PhoQ. The gene feedback loop for PhoP/PhoQ expression in (**C**) wild-type and (**D**) mutant strains. (**E**) The normalized P-PhoP level in wild-type strain. The blue dashed line defines the surge height H. (**F**) Occupancy of the pmrD promoters by PhoP and P-PhoP. (**G**) The normalized mRNA expression of pmrD. The symbols ↔ and → denote the reversible and irreversible reactions, respectively. Solid arrows represent the forward reactions, and hollow arrows represent the backward reactions. Black squares and red circles represent the experimental data in wild-type and mutant strains, respectively. Black and red lines represent the simulated results of the wild-type and the mutant models, respectively. The ordinate unit is the arbitrary unit (a.u.). (Color version of this figure is available at *Bioinformatics* online.)

three stages, including the increasing phase in the first and second stages (P1 and P2), and the decreasing phase in the third stage (P3). The increasing stage P1 starts right after stimulation. The initial proteins of PhoQ rapidly autophosphorylates into P-PhoQ through P-PhoQ-ADP [Fig. 2A(b1, c, d)]. When all the initial proteins of PhoP [Fig. 2B(b)] in the system are phosphorylated by P-PhoQ through P-PhoQ-PhoP complex [Fig. 2A(e)], giving the first stage with a character of increasing P-PhoP [Fig. 2B(f)]. The P-PhoP is also contributed in the phosphorylation reaction of P-PhoQ-ADP with PhoP [Fig. 2B(c)]. The P1 stage is ended when the initial PhoP level of approximately $2.7\mu M$ is completely depleted and converted into P-

PhoP [the red arrow in Fig. 2B(b)], while the initial PhoQ level is also completely phosphorylated into P-PhoQ [the red arrow in Fig. 2A(b1)]. As a result, the P1 stage right after stimulation is defined as the stress response period. The major signal pathway in such a stage is summarized in Supplementary Figure S1A.

Furthermore, P-PhoP could promote the expression of PhoP and PhoQ, which is generated by DNA bound by P-PhoP as a positive gene feedback loop. It is notable that the total amount of all types of PhoQ proteins (including free PhoQ and all PhoQ complexes) have slight increases in concentration because the balance between PhoQ protein generation and degradation is broken right after stimulation
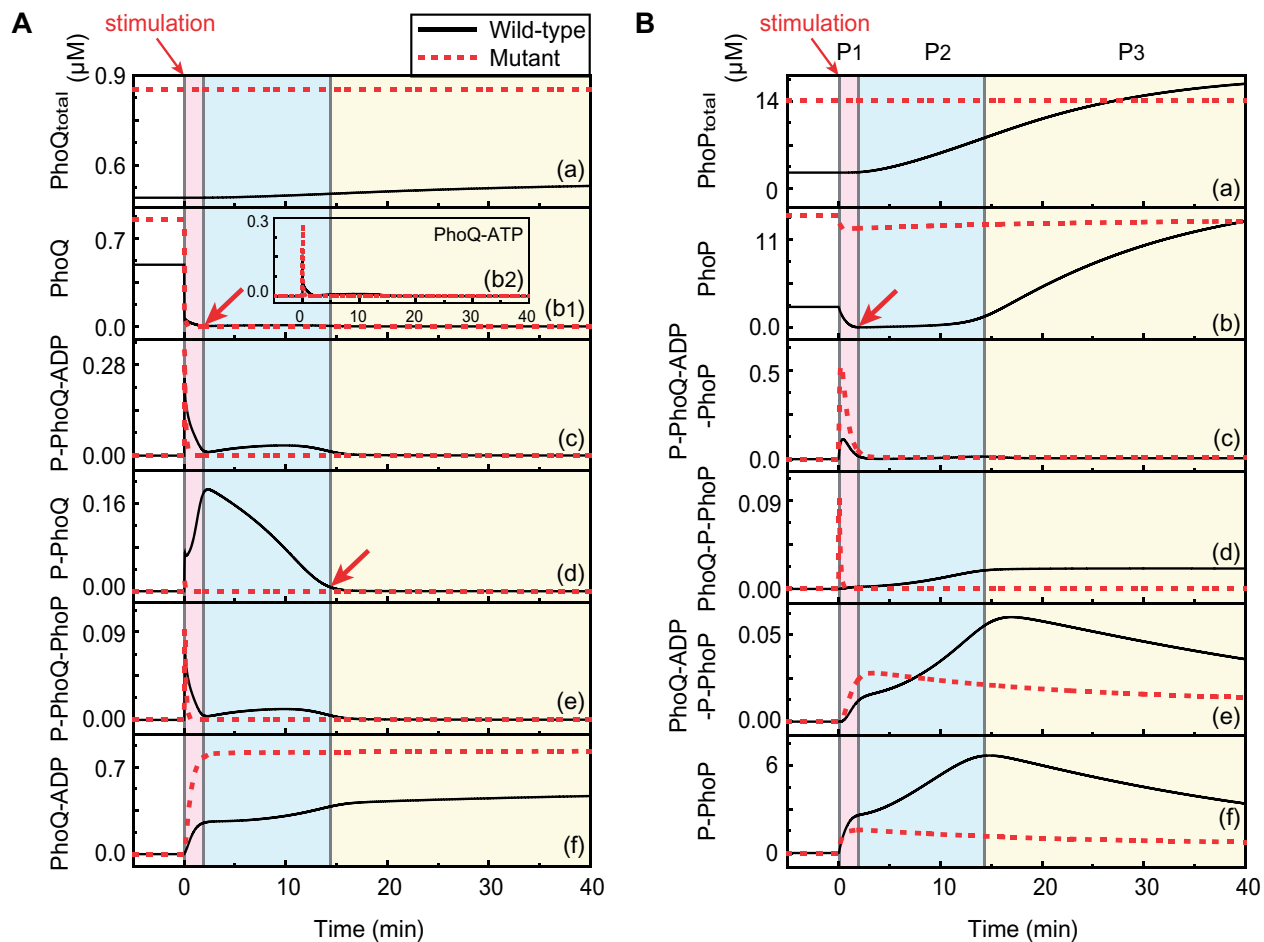
Fig. 2. Dynamics of the three stages of the surge observed in wild-type strain. (**A**, **B**) Profiles of key components in response to stimulation. Black solid lines represent the dynamic levels in wild-type model, while red dotted lines represent the levels in mutant model. The gray solid lines divide three stages, and the red arrows indicate the key proteins in the transition between the two stages. (Color version of this figure is available at *Bioinformatics* online.)

[Fig. 2A(a)]. In contrast, the total amount of all types of PhoP proteins starts to increase significantly in P2 stage [Fig. 2B(a)]. The newly produced PhoP is phosphorylated rapidly by P-PhoQ that further increases the P-PhoP level [Fig. 2A(d) and B(f)], giving the occurrence of the second peak of P-PhoQ-PhoP [Fig. 2A(e)]. The second stage is ended when P-PhoP reaches its maximal due to the exhausted P-PhoQ [the red arrow in Fig. 2A(d)]. Thus, the second stage can be called the gene feedback period to produce more PhoP for phosphorylation. The major signal pathway in P2 is summarized in Supplementary Figure S1B.

In P3 stage, the amount of P-PhoP becomes descending. The free PhoQ and its complexes, including P-PhoQ, P-PhoQ-ADP, PhoQ-ATP, P-PhoQ-PhoP and P-PhoQ-ADP-PhoP, are all exhausted [see Fig. 2A(b1, b2, c, d, e) and B(c)], resulting in a termination of reactions in signal pathways of Supplementary Figure S1A and B. Specifically, P-PhoP is converted into PhoP through interactions with PhoQ-ADP, driving P-PhoP to descend to a steady state [Figs. 2A(f) and B(e, f)]. Therefore, this stage is referred to the dephosphorylation period by PhoQ-ADP. The corresponding signal reaction pathway is plotted in Supplementary Figure S1C. As a result, these three dynamic stages form the P-PhoP surge.

However, in the mutant model the constitutive expression of PhoP and PhoQ results in high levels of PhoP and PhoQ before stimulation (Shin *et al.*, 2006) [the red dotted lines in Fig. 2A(b1) and B(b)]. In low Mg^{2+}, PhoP is rapidly phosphorylated to P-PhoP by P-PhoQ-ADP and P-PhoQ, leading to an increase of P-PhoP, which is similar to the stress response period after stimulation observed in the wild-type model. Next, due to a constant PhoQ concentration, the free PhoQ and its complexes, including PhoQ-ATP,

P-PhoQ-ADP, P-PhoQ, P-PhoQ-PhoP, P-PhoQ-ADP-PhoP and PhoQ-P-PhoP, are all exhausted rapidly [Fig. 2A(b1, b2, c, d, e) and B(c, d)]. Such an exhausted state leads the mutant strain directly to the dephosphorylation period by PhoQ-ADP without the surge (Fig. 2A and B).

3.2 The mechanism of surge caused by the ADP affinity of PhoQ

As observed in experiment, the P-PhoP level became substantially higher and was sustained longer when the affinity of PhoQ and ADP was decreased (Yeo *et al.*, 2012). Consistently, the decrease of the association rate of PhoQ and ADP (i.e. k_{12}) enhances the surge in the wild-type model (Fig. 3A and Supplementary Fig. S2). The qualitative reproduction of the experimental results verifies the rationality of the model. Figure 3A shows the time-dependent responses of P-PhoP, P-PhoQ and PhoQ-ADP with three typical association rates of PhoQ and ADP, which are marked by dotted lines in Supplementary Figure S2. The decreased association rate of PhoQ and ADP (i.e. k_{12}) directly results in an increase of PhoQ, which enhances the P-PhoP generation through phosphorylation process. And at the same time, the decreased association rate directly causes a reduction of PhoQ-ADP, which reduces the dephosphorylation of P-PhoP (Fig. 3A). Thus, these two processes both increase the surge of P-PhoP.

As a result, the surge height H is plotted as functions of the association and dissociation rates of PhoQ and ADP in Figure 3B and C, respectively, showing a behavior of sigmoidal curve. The related primary signal pathways for surge caused by the ADP affinity of PhoQ
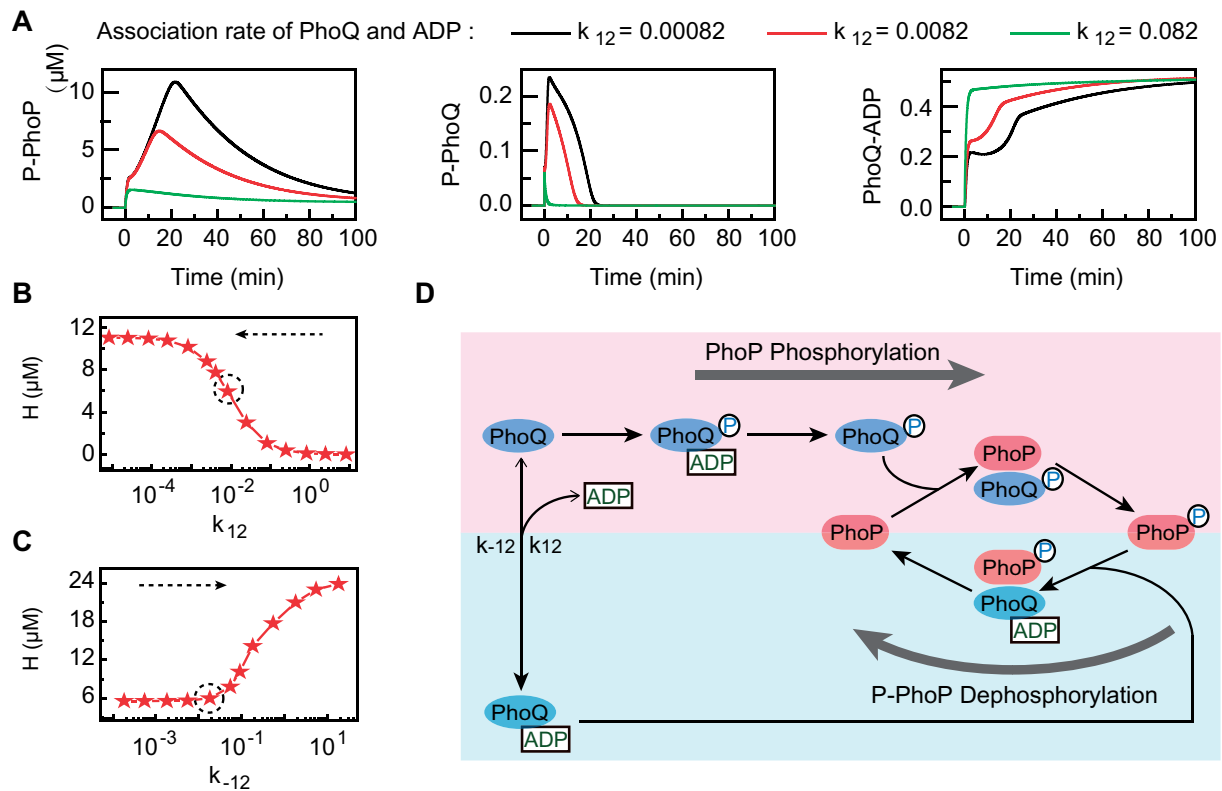
Fig. 3. The mechanism of surge caused by the ADP affinity of PhoQ. (**A**) The dynamic profiles of P-PhoP (left panel), P-PhoQ (middle panel) and PhoQ-ADP (right panel) complexes corresponding to the three association rates of PhoQ and ADP at k_{12} =0.0082 (red), 0.00082 (black) and 0.082 (green) (the three-dotted lines in Supplementary Fig. S2), respectively. The surge height H plotted with (**B**) the association rate k_{12} and (**C**) the dissociation rate k_{-12} of PhoQ and ADP. The stars with the dotted circle correspond to the standard model at k_{12} =0.0082. The black dotted arrows indicate a reduction direction of the ADP affinity with PhoQ. (**D**) Primary signal pathways for surge caused by the ADP affinity of PhoQ. (Color version of this figure is available at *Bioinformatics* online.)

are summarized in Figure 3D, in which the pink and cyan areas describe the PhoP phosphorylation and the P-PhoP dephosphorylation processes, respectively.

3.3 The P-PhoP-promoting and P-PhoP-depressing pathways

In order to investigate the modulation mechanism of the P-PhoP surge systematically, we perform the perturbation analysis for all parameters in the wild-type model. The individual reaction rate is given by λk_i with the standard parameter k_i multiplied by a scale λ to modulate the reaction process in the model. Simulation results show that, as the multiplication scale λ increases for individual reaction rate, the surge of P-PhoP will either increase (e.g. the association rate of PhoQ and ATP k_1), decrease (e.g. the association rate of P-PhoQ-ADP and PhoP k_4) or remain unchanged (e.g. the dissociation rate of PhoQ and ATP k_{-1}), respectively (Supplementary Fig. S3A and B). According to the influence of parameter perturbation on surge height H, the reaction parameter in the signaling pathways can be classified into three categories: (i) parameters to promote P-PhoP, (ii) parameters to depress P-PhoP and (iii) the insensitive parameters with little effect on P-PhoP (Fig. 4A).

As a result, the P-PhoP-promoting and P-PhoP-depressing signal pathways are summarized in Figure 4B. Clearly, the P-PhoP-promoting pathways (reactions with red lines in Fig. 4B) consist of both the PhoQ phosphorylation reactions and the PhoP phosphorylation reactions. Such P-PhoP-promoting signaling pathway acts as a source to generate P-PhoP. And the depressing pathway mainly dephosphorylates P-PhoP to PhoP and deplete P-PhoP (i.e. the reactions with green lines in Fig. 4B). Furthermore, the P-PhoQ-ADP and P-PhoQ-ADP-PhoP reactions with parameters k_4 and k_{-4} typically play a leaking role to drain P-PhoQ-ADP away from the P-PhoP-promoting pathway. As a result, the competition between the

P-PhoP-promoting and the P-PhoP-depressing pathways determine the generation of surge. Both PhoP and PhoQ are not only in the P-PhoP-promoting reaction pathway, but also in the P-PhoP-depressing reaction pathway, thereby playing bifunctional roles in the surge modulation.

3.4 Biphasic regulation of PhoP and PhoQ expressions on the surge

The normalized surge height H as a function of multiplication scale for the reaction parameters in gene feedback loop shown in Figure 1C increases firstly to a maximum, and then decreases (Fig. 5A and B). For example, the dynamic profiles of P-PhoP protein with the varying multiplication scale λ for the translation rates of PhoQ (k_{19}) and PhoP (k_{18}) both present an area of high P-PhoP level in the middle region (Supplementary Fig. S4A and B). This bell-shaped phenomenon indicate a biphasic regulation of reactions in gene feedback loop on the P-PhoP surge. The kinetic behaviors of the components associated with the P-PhoP surge are plotted with three different translation rates of PhoQ from mRNA (k_{19}) (Fig. 5C, corresponding to the three-dotted lines in Supplementary Fig. S4A). When the PhoQ translation rate increases to $100*k_{19}$ from the standard value k_{19}, the increasing PhoQ causes more PhoP phosphorylation. The P-PhoP-promoting reactions dominate the system with an enhanced surge (the red line in Fig. 5C). However, when k_{19} turns to $1000*k_{19}$, the overfilled PhoQ either directly interacts with P-PhoP to dephosphorylate P-PhoP or recruits ADP (i.e. PhoQ-ADP) to rapidly dephosphorylate P-PhoP (the green lines in Fig. 5C). As a result, large amounts of PhoQ and PhoQ-ADP dominate the P-PhoP-depressing reactions, causing a small P-PhoP surge.

The kinetic behaviors of the components associated with the P-PhoP surge are plotted with three different translation rates of PhoP from mRNA (k_{18}) (Fig. 5D, corresponding to the three-dotted lines in

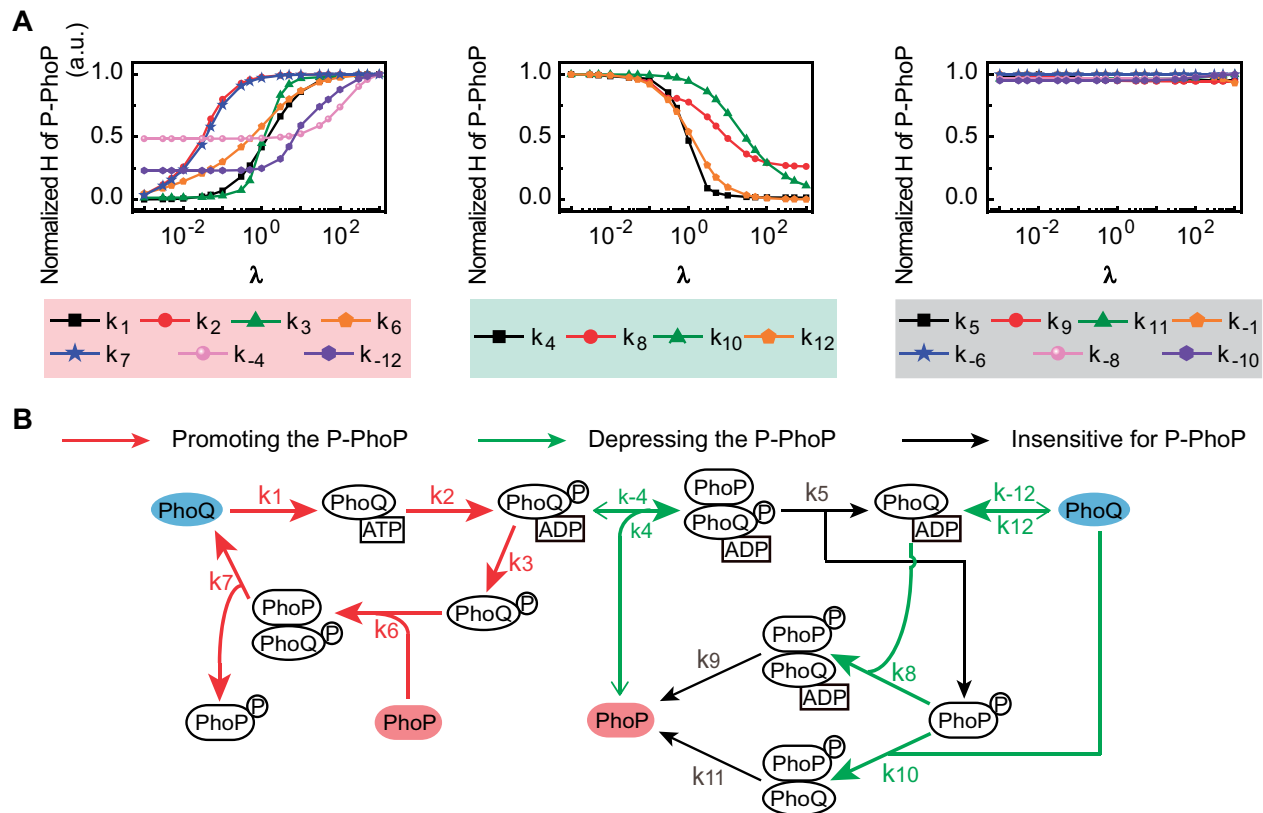**Fig. 4.** The perturbation analyses of parameters in the PhoP/PhoQ signal pathways. (**A**) The normalized surge height H plotted against the multiplication scale λ for all reaction rates in Figure 1B. All the reaction rates are classified into three categories: parameters to promote P-PhoP (left panel), parameters to depress P-PhoP (middle panel) and the insensitive parameters for P-PhoP (right panel). (**B**) The related P-PhoP-promoting pathways (red lines) and P-PhoP-depressing pathways (green lines) for the PhoP/PhoQ signaling. The black lines represent the parameters that are insensitive for P-PhoP. (Color version of this figure is available at *Bioinformatics* online.)

Supplementary Fig. S4B). The increase of PhoP translation rate from $0.001*k_{18}$ to k_{18} results in the increase of P-PhoP, which generates the surge (red line in Fig. 5D). However, with a larger PhoP production rate of $1000*k_{18}$, the excessive PhoP typically drives P-PhoQ-ADP to become P-PhoQ-ADP-PhoP. In the absence of P-PhoQ and P-PhoQ-ADP, the P-PhoP-promoting reaction is terminated and results in a weakened surge (green lines in Fig. 5D) along with a PhoP accumulation. Therefore, the bifunctional roles of PhoP and PhoQ in the P-PhoP generation give rise to a biphasic regulation on the P-PhoP surge for the reaction processes in gene feedback loop.

The transcription rate of mRNA (k_{16}) is also an important parameter in the gene feedback loop. The normalized surge height H as a function of multiplication scale of transcription rate of mRNA is plotted in Figure 5B. One can see that its modulation behavior on surge height is similar as that of the translation rates of PhoP (k_{18}), both giving a biphasic surge height. The corresponding kinetic behaviors of P-PhoP, PhoP, P-PhoQ and P-PhoQ-ADP are given in Supplementary Figure S4C, D.

It has been suggested that the surge phenomenon is dominated by the negative feedback loop or incoherent feedforward loop (Ferrell, 2016). Based on our PhoP/PhoQ TCS, there are three modulation structures as the primary signaling pathways that are correlated with P-PhoP. The left and middle panels in Figure 5E display the primary pathways of promoting and suppressing P-PhoP by PhoQ, respectively. While the right panel in Figure 5E displays the primary pathways of promoting PhoP and PhoQ by stimulating the gene expression. The incoherent feedforward loops are formed by combining the left and middle primary pathways. Meanwhile, the negative feedback loops are formed by combining the middle and right primary pathways. Additionally, the analysis of parameter sensitivity (Supplementary Fig. S5) shows that all the parameters that the surge of P-PhoP is sensitive to (Fig. 5F) belong to the promoting (the left panel of Fig. 5E) and depressing (the middle panel of Fig. 5E) P-PhoP pathways. Therefore,

we conclude that the formation of the surge is a result of the interactions of these incoherent feedforward and negative feedback loops.

4 Discussion

The transcriptional surge has been considered as a general characteristics in TCS families, which is essential for the regulation of various physiological functions in bacteria (Ray and Igoshin, 2010; Shin *et al.*, 2006). A decade of experimental and modeling studies (Batchelor and Goulian, 2003; Locke *et al.*, 2011; Mitrophanov *et al.*, 2010; Qin *et al.*, 2001; Ray and Igoshin, 2010; Salazar *et al.*, 2016; Shin *et al.*, 2006; Tzeng and Hoch, 1997; Yeo *et al.*, 2012) suggests that a positive gene feedback plays an important role to cause the P-PhoP surge (Shin *et al.*, 2006), while the ADP-binding affinity of PhoQ serves as a key factor to a negative feedback loop (Yeo *et al.*, 2012).

We have investigated the generation mechanism of surge by using a comprehensive mathematical modeling of the TCS PhoP/PhoQ in the paper. Our model is able to nicely recapitulate the two experimental results for surge generation (Shin *et al.*, 2006; Yeo *et al.*, 2012). We suggest that the P-PhoP surge in wild-type strain can be divided into three stages, including the stress response period in which all the initial proteins of PhoP in the system are phosphorylated to P-PhoP, the gene feedback period in which the PhoP proteins generated by the gene feedback loop are further phosphorylated to P-PhoP, both giving the increasing phase of P-PhoP surge, and the dephosphorylation period of P-PhoP, resulting in the decreasing phase of P-PhoP surge. However, in the mutant model due to the high constitutive expression of PhoP and PhoQ, PhoP is rapidly phosphorylated to P-PhoP by P-PhoQ-ADP and P-PhoQ, forming the stress response period after stimulation. Next, owing to the absence of gene feedback loop, the level of P-PhoP is
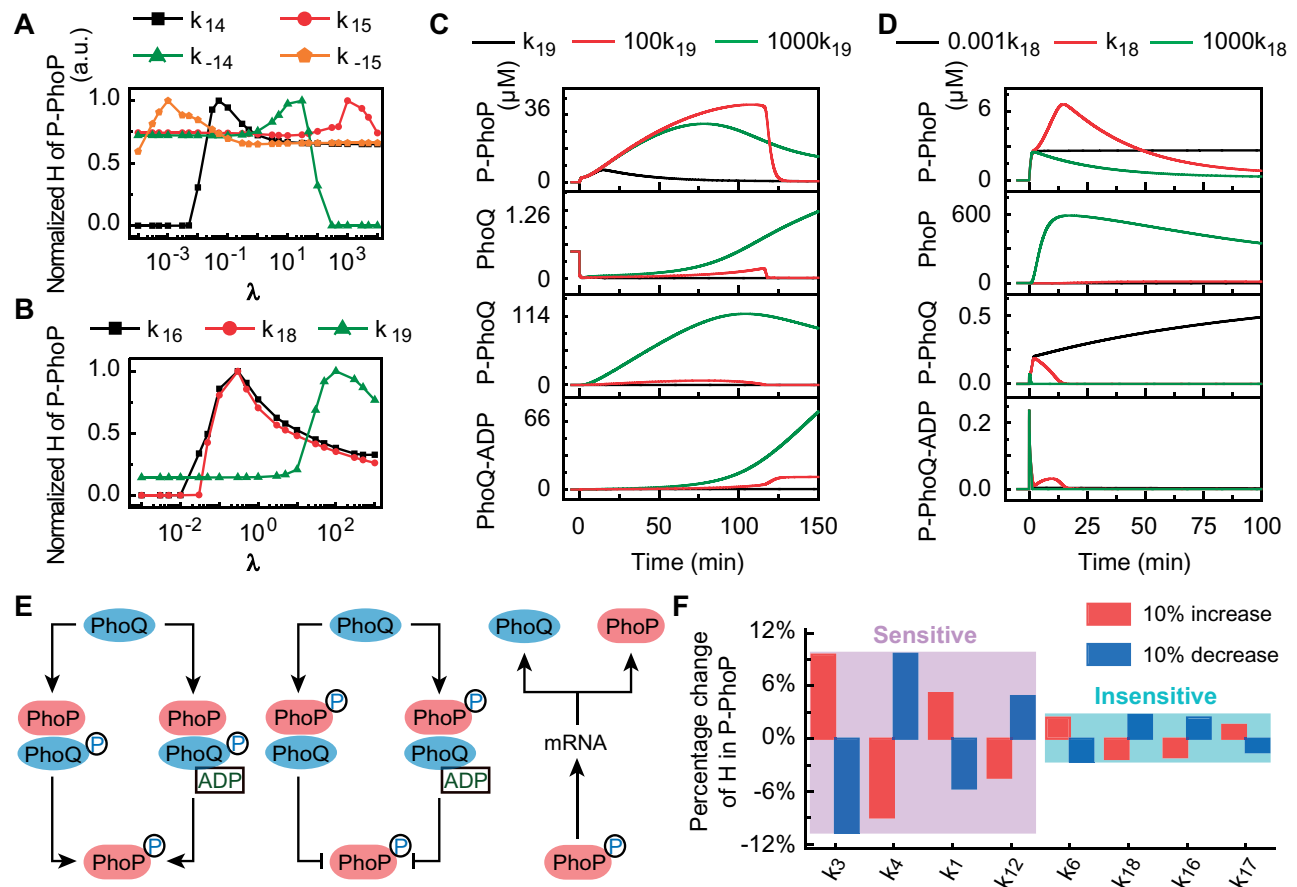
Fig. 5. The perturbation analysis of parameters in the PhoP/PhoQ expression loop. The normalized surge height H of P-PhoP with the increase of multiplication scale (**A**) for all the reaction rates of PhoP/P-PhoP binding to DNA, and (**B**) for the three parameters for transcription and PhoP/PhoQ translations in DNA feedback loop, all giving a biphasic behavior of height H. (**C**) The kinetic plots of P-PhoP, PhoQ, P-PhoQ and PhoQ-ADP at the three specific translation rates of PhoQ from mRNA (i.e. k_{19}, the three-dotted lines in Supplementary Fig. S4A). (**D**) Kinetic plots of P-PhoP, PhoP, P-PhoQ and P-PhoQ-ADP at the three specific translation rates of PhoP from mRNA (i.e. k_{18}, the three-dotted lines in Supplementary Fig. S4B). (**E**) The three primary topological structures that correlate with P-PhoP signal pathways: two pathways of promoting (left panel) and depressing (middle panel) P-PhoP by PhoQ, respectively, and the pathway of promoting PhoP and PhoQ by stimulating the gene expression (right panel). (**F**) Percentage change of the surge height H in P-PhoP in response to 10% increase (red bar) or 10% decrease (blue bar) of the sensitive parameters (in purple box) (see Supplementary Fig. S5 for detail). As a comparison, results for some insensitive parameters are also displayed (in the cyan box). (Color version of this figure is available at *Bioinformatics* online.)

directly dephosphorylated by PhoQ-ADP without the occurrence of surge (Fig. 2A and B).

Generally we have identified two major pathways, i.e. P-PhoP-promoting and P-PhoP-depressing pathways, for the P-PhoP surge. The P-PhoP-promoting pathways consist of the PhoQ phosphorylation and PhoP phosphorylation reactions (red lines in Fig. 4B), which act as a source to generate P-PhoP. The P-PhoP-depressing pathways consist of the P-PhoP depleting and P-PhoQ-ADP kinase activity draining reactions (green lines in Fig. 4B). Thus, the competition between the P-PhoP-promoting and the P-PhoP-depressing pathways determines the generation of P-PhoP surge. By varying the affinity rate of these two pathways, one could be able to modulate the surge of P-PhoP and further affect the virulence of bacteria, which are consistent with the results of (Gunn *et al.*, 1996; Miller and Mekalanos, 1990; Yeo *et al.*, 2012).

As a bifunctional protein, PhoQ can promote the phosphorylation of its cognate PhoP in kinase state and dephosphorylate its cognate P-PhoP in phosphatase state (Yang and Inouye, 1991; Yeo *et al.*, 2012). Our modeling studies further reveal that PhoP is also a bifunctional protein on the P-PhoP modulation. PhoP can be directly phosphorylated by P-PhoQ to P-PhoP and drain the kinase state P-PhoQ-ADP by interacting with it, causing the depressing of P-PhoP generation reactions (green lines in Fig. 4B). As a result, the bifunctional roles of PhoP and PhoQ in the P-PhoP generation can generate a biphasic regulation of the P-PhoP surge by the reaction processes in the gene feedback loop (Fig. 5). Generally, we propose that the

bifunctional modulation of RR and HK on P-RR may lead to a biphasic regulation of the gene feedback loops on the surge, not only for TCSs when the molecule number of RR is larger than HK (Groisman, 2016), but also for those TCSs that the molecule number of HK is larger than RR, such as the LiaFSR system (Karen *et al.*, 2013).

Our study also confirmed that the generation of the surge is a result of the interactions of the incoherent feedforward and negative feedback loops, as suggested by (Ferrell, 2016). Furthermore, we predict that the mechanisms for the surge by PhoP/PhoQ may be applied for other TCSs in which the gene feedback loops are even absent (Fig. 6), e.g. VicK/VicR (Gotoh *et al.*, 2010). Although there is a lack of negative feedback loops in TCSs without gene feedback loops, there are still some incoherent feedforward loops formed by the primary pathways of promoting and suppressing P-PhoP by PhoQ (left and middle panels in Fig 5E). In details, in such TCS the pathways of HK-phosphorylation (red lines in Fig. 6) and RR-phosphorylation (purple lines in Fig. 6) which promote P-RR, and the P-RR dephosphorylating pathway (blue lines in Fig.6) and the leaking pathway to drain the kinase state P-HK-ADP (cyan lines in Fig. 6) which decrease P-RR constitute the incoherent feedforward loops, which can generate the P-RR surge.

Compared to the biologically realistic system, our TCS network is a very abstract model. It is worth to note that a small protein MgrB can inhibit the PhoP/PhoQ to mediate the surge by establishing a negative feedback loop (Salazar *et al.*, 2016). Similar as
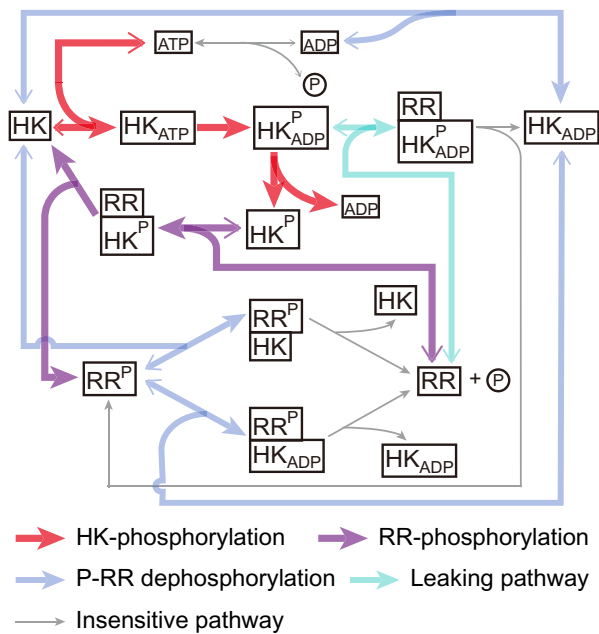
Fig. 6. General mechanism for the P-RR surge in TCS even without gene feedback loop. The HK-phosphorylation pathway (red lines) and RR-phosphorylation pathway (purple lines) promote P-RR. The P-RR dephosphorylating pathway (blue lines) and the leaking pathway to drain the kinase state P-HK-ADP (cyan lines) decrease P-RR. The gray lines indicate the insensitive pathway. (Color version of this figure is available at *Bioinformatics* online.)

magnesium, calcium was also found to be able to induce PhoP/PhoQ in the TCS system (Groisman, 2001). Additionally, the mildly acidic pH can enhance PhoQ to autophosphorylate and further promote transcription of mRNA (Choi and Groisman, 2017). Therefore, a more realistic model could be established by involving these players in the future. Meanwhile, we made predictions about the effects of the changes of reaction rates and translation rates on surge height with the model and some new insights are provided on the surge dynamics by this study. Although it is a challenge to change the reaction rate in experiments, we hope that our predictions can be tested by future experiment. We also suggest that the mechanisms derived from the PhoP/PhoQ for the transcriptional surges may aid to develop new antimicrobial strategies targeting TCSs.

Acknowledgements

Funding

References

Alloing,G. *et al.* (1998) Development of competence in streptococcus pneumoniae: pheromone autoinduction and control of quorum sensing by the oligopeptide permease. *Mol. Microbiol.*, **29**, 75–83.

Batchelor,E. and Goulian,M. (2003) Robustness and the cycle of phosphorylation and dephosphorylation in a two-component regulatory system. *Proc. Natl. Acad. Sci. USA*, **100**, 691–696.

Castelli,M.E. *et al.* (2000) The phosphatase activity is the target for mg2+ regulation of the sensor protein phoq in salmonella. *J. Biol. Chem.*, **275**, 22948–22954.

Chang,C. and Stewart,R.C. (1998) The two-component system regulation of diverse signaling pathways in prokaryotes and eukaryotes. *Plant Physiol.*, **117**, 723–731.

Choi,J. and Groisman,E.A. (2017) Activation of master virulence regulator phop in acidic pH requires the salmonella-specific protein UGTL. *Sci. Signal.*, **10**, eaan6284.

Dutta,R. *et al.* (1999) Histidine kinases: diversity of domain organization. *Mol. Microbiol.*, **34**, 633–640.

Ferrell,J. (2016) Perfect and near-perfect adaptation in cell signaling. *Cell Syst.*, **2**, 62–67.

Gao,R. *et al.* (2007) Bacterial response regulators: versatile regulatory strategies from common domains. *Trends Biochem. Sci.*, **32**, 225–234.

Garcia Vescovi,E. *et al.* (1996) Mg2+ as an extracellular signal: environmental regulation of *Salmonella* virulence. *Cell*, **84**, 165–174.

Gotoh,Y. *et al.* (2010) Two-component signal transduction as potential drug targets in pathogenic bacteria. *Curr. Opin. Microbiol.*, **13**, 232–239.

Groisman,E.A. (2001) The pleiotropic two-component regulatory system phop-phoq. *J. Bacteriol.*, **183**, 1835–1842.

Groisman,E.A. (2016) Feedback control of two-component regulatory systems. *Annu. Rev. Microbiol.*, **70**, 103–124.

Guckes,K.R. *et al.* (2017) Signaling by two-component system noncognate partners promotes intrinsic tolerance to polymyxin b in uropathogenic escherichia coli. *Sci. Signal.*, **10**, eaag1775.

Gunn,J.S. *et al.* (1996) Transcriptional regulation of salmonella virulence: a phoq periplasmic domain mutation results in. *J. Bacteriol.*, **178**, 6369–6369.

Hess,J.F. *et al.* (1988) Phosphorylation of three proteins in the signaling pathway of bacterial chemotaxis. *Cell*, **53**, 79–87.

Hutchings,M.I. *et al.* (2006) The vancomycin resistance vanrs two-component signal transduction system of *Streptomyces coelicolor*. *Mol. Microbiol.*, **59**, 923–935.

Igo,M.M. *et al.* (1989) Phosphorylation and dephosphorylation of a bacterial transcriptional activator by a transmembrane receptor. *Genes Dev.*, **3**, 1725–1734.

Jason,K. *et al.* (2007) Time-resolved crystallographic studies of the heme domain of the oxygen sensor fixl: structural dynamics of ligand rebinding and their relation to signal transduction. *Biochemistry*, **46**, 4706.

Karen,S. *et al.* (2013) Stoichiometry and perturbation studies of the liafsr system of *Bacillus subtilis*. *Mol. Microbiol.*, **87**, 769–788.

Kato,A. *et al.* (1999) Molecular characterization of the phop-phoq two-component system in escherichia coli k-12: identification of extracellular mg2+-responsive promoters. *J. Bacteriol.*, **181**, 5516–5520.

Krell,T. *et al.* (2010) Bacterial sensor kinases: diversity in the recognition of environmental signals. *Annu. Rev. Microbiol.*, **64**, 539–559.

Lejona,S. *et al.* (2003) Molecular characterization of the mg2+-responsive phop-phoq regulon in *Salmonella enterica*. *J. Bacteriol.*, **185**, 6287–6294.

Li,X. *et al.* (2020) Data-driven modeling identifies tirap-independent myd88 activation complex and myddosome assembly strategy in lps/tlr4 signaling. *Int, J, Mol. Sci.*, **21**, 3061.

Li,X. *et al.* (2021) Rip1-dependent linear and nonlinear recruitments of caspase-8 and rip3 respectively to necrosome specify distinct cell death outcomes. *Protein Cell*, 1-19.

Locke,J.C. *et al.* (2011) Stochastic pulse regulation in bacterial stress response. *Science*, **334**, 366–369.

Mascher,T. *et al.* (2006) Stimulus perception in bacterial signal-transducing histidine kinases. *Microbiol. Mol. Biol. Rev.*, **70**, 910–938.

Miller,S.I. and Mekalanos,J.J. (1990) Constitutive expression of the phop regulon attenuates salmonella virulence and survival within macrophages. *J. Bacteriol.*, **172**, 2485–2490.

Mitrophanov,A.Y. *et al.* (2010) Positive autoregulation shapes response timing and intensity in two-component signal transduction systems. *J. Mol. Biol.*, **401**, 671–680.

Ninfa,A.J. and Magasanik,B. (1986) Covalent modification of the glng product, nri, by the glnl product, nrii, regulates the transcription of the glnalg operon in escherichia coli. *Proc. Natl. Acad. Sci. USA*, **83**, 5909–5913.

Perraud,A.L. *et al.* (1999) Signalling pathways in two-component phosphorelay systems. *Trends Microbiol.*, **7**, 115–120.

Pestova,E.V. *et al.* (1996) Regulation of competence for genetic transformation in streptococcus pneumoniae by an auto-induced peptide pheromone and a two-component regulatory system. *Mol. Microbiol.*, **21**, 853–862.

Qi,H. *et al.* (2015) Optimal microdomain crosstalk between endoplasmic reticulum and mitochondria for ca2+ oscillations. *Sci. Rep.*, **5**, 7984.

Qi,H. *et al.* (2018) Optimal pathways for the assembly of the apaf-1 cyto-chrome c complex into apoptosome. *Phys. Chem. Chem. Phys. PCCP*, **20**, 1964–1973.

Qin,L. *et al.* (2001) The critical role of dna in the equilibrium between ompr and phosphorylated ompr mediated by envz in *Escherichia coli*. *Proc. Natl. Acad. Sci. USA*, **98**, 908–913.

Ray,J.C. and Igoshin,O.A. (2010) Adaptable functionality of transcriptional feedback in bacterial two-component systems. *PLoS Comput. Biol.*, **6**, e1000676.

Robinson,V. *et al.* (2000) A tale of two components: a novel kinase and a regu-latory switch. *Nat. Struct. Biol.*, **7**, 626–633.

Salazar,M.E. *et al.* (2016) The small membrane protein mgrb regulates phoq bifunctionality to control phop target gene expression dynamics. *Mol. Microbiol.*, **102**, 430–445.

Shin,D. and Groisman,E.A. (2005) Signal-dependent binding of the response regulators phop and pmra to their target promoters in vivo. *J. Biol. Chem.*, **280**, 4089–4094.

Shin,D. *et al.* (2006) A positive feedback loop promotes transcription surge that jump-starts salmonella virulence circuit. *Science*, **314**, 1607–1609.

Stock,A.M. *et al.* (2000) Two-component signal transduction. *Annu. Rev. Biochem.*, **69**, 183–215.

Straube,R. (2014) Reciprocal regulation as a source of ultrasensitivity in two-component systems with a bifunctional sensor kinase. *PLoS Comput. Biol.*, **10**, e1003614.

Tzeng,Y.L. and Hoch,J.A. (1997) Molecular recognition in signal transduc-tion: the interaction surfaces of the spo0f response regulator with its cognate phosphorelay proteins revealed by alanine scanning mutagenesis. *J. Mol. Biol.*, **272**, 200–212.

Williams,S.B. and Stewart,V. (1997) Nitrate- and nitrite-sensing protein narx of escherichia coli k-12: mutational analysis of the amino-terminal tail and first transmembrane segment. *J. Bacteriol.*, **179**, 721–729.

Wuichet,K. *et al.* (2010) Evolution and phyletic distribution of two-component signal transduction systems. *Curr. Opin. Microbiol.*, **13**, 219–225.

Yamamoto,K. and Ishihama,A. (2005) Transcriptional response of *Escherichia coli* to external copper. *Mol. Microbiol.*, **56**, 215–227.

Yamamoto,K. *et al.* (2002) Novel mode of transcription regulation of diver-gently overlapping promoters by phop, the regulator of two-component sys-tem sensing external magnesium availability. *Mol. Microbiol.*, **45**, 423–438.

Yang,Y. and Inouye,M. (1991) Intermolecular complementation between two defective mutant signal-transducing receptors of *Escherichia coli*. *Proc. Natl. Acad. Sci. USA*, **88**, 11057–11061.

Yeo,W.S. *et al.* (2012) Intrinsic negative feedback governs activation surge in two-component regulatory systems. *Mol. Cell*, **45**, 409–421.